

Electronic Structure of B-2p State in AlB₂ Single Crystal: Direct Observation of $p\sigma$ and $p\pi$ Density of States

Jin NAKAMURA^{*}, Masamitsu WATANABE¹, Tamio OGUCHI², Sin-ya NASUBIDA,
Eiki KABASAWA, Nobuyoshi YAMADA, Kazuhiko KUROKI, Hisashi YAMAZAKI,
Shik SHIN³, Yuji UMEDA⁴, Shin MINAKAWA⁴,
Noriaki KIMURA⁴ and Haruyoshi AOKI⁴

*Department of Applied Physics and Chemistry, The University of Electro-Communications,
Chofu, Tokyo 182-8585*

¹RIKEN/Spring-8, Kouto 1-1-1, Mikazuki, Sayo, Hyogo 679-5148

²Department of Quantum Matter, ADSM, Hiroshima University, Higashihiroshima, Hiroshima 739-8530

³The Institute for Solid State Physics, The University of Tokyo, Kashiwa, Chiba 277-8581

⁴Center for Low Temperature Science, Tohoku University, Sendai 980-8578

(Received November 27, 2001)

X-ray emission (XES) and absorption (XAS) spectra near the B-K edge were measured on single-crystalline AlB₂ compound which is an isostructural diboride of superconducting MgB₂. The partial density of states (PDOS) of B-2p σ and $p\pi$ orbitals were derived from the polarization dependence of XES and XAS spectra. There are considerable amounts of PDOS near the Fermi energy in AlB₂ similarly to that in MgB₂, but there are almost no PDOS in $p\sigma$ orbitals of AlB₂ near the Fermi energy, i.e., a pseudo-gap in $p\sigma$ state and a broad metallic state in $p\pi$ state are observed. The present result indirectly supports scenarios that the $p\sigma$ holes play an important role in the occurrence of superconductivity in MgB₂. The overall features of PDOS were found to be in good agreement with the result of band calculation of AlB₂, but a small discrepancy in the Fermi energy is observed, which is attributed to the Al vacancy in the compounds, i.e., the estimated concentration is Al_{0.93}B₂.

KEYWORDS: MgB₂, AlB₂, single crystal, partial density of state, $p\sigma$ and $p\pi$ orbitals, X-ray emission and absorption spectroscopy
DOI: 10.1143/JPSJ.71.408

Since the discovery of superconductivity in MgB₂ with a transition temperature, T_c , of 39 K by Nagamatsu *et al.*,¹⁾ a large number of research studies from experimental^{2–4)} and theoretical^{5–14)} points of view have been performed on this compound and on a series of isostructural diborides. In a previous paper,⁴⁾ we reported a large partial density of states (PDOS) of B-2p orbitals near the Fermi energy, E_F , in MgB₂ by soft X-ray emission (XES) and absorption spectroscopies (XAS) near the B-K edge. This result is consistent with the results of band calculations, which suggest the holes in $p\sigma$ bands between B–B in a honeycomb plane play important roles in the superconductivity of MgB₂. Although there are many experimental results that suggest MgB₂ is considered as an s-type superconductor with a strong electron-phonon coupling, the reason for the high value of T_c as a conventional BCS-type superconductor is not clear. An efficient step towards understanding the mechanism of superconductivity in MgB₂ is to clarify the difference between this material and other materials which have the same crystal structure but are not superconductors. An example of such materials is AlB₂. From a theoretical point of view, first principles band calculations reveal that a large difference between MgB₂ and AlB₂ is that the Fermi level intersects the 2p σ band in the former, while it does not in the latter, suggesting that the $p\sigma$ band plays an important role in the occurrence of superconductivity in MgB₂.^{9,15)} However, until now, a direct experimental confirmation that such band-calculation predictions are indeed correct has not yet been reported.

To clarify this point, here we directly observe the PDOS

of B-2p σ and 2p π bands in AlB₂ by performing polarization-dependent XES and XAS on a single crystalline compound. The single-crystalline AlB₂ samples were prepared by the Al-flux method. Mixtures of Al (purity, 4N) and B (purity, 4N5) powders were placed in an Al₂O₃ crucible and heated in an Ar gas atmosphere up to 1000°C, and then cooled slowly to 660°C. The synthesized AlB₂ single crystals were separated from the solidified melts by dissolving the Al flux with sodium hydroxide solution. The obtained crystals resemble a hexagonal plate with the edge length (in *ab*-plane) of about 1–2 mm and with the thickness of about 10 μ m along the *c*-axis. Before XES and XAS measurements, the crystal was polished in order to remove Al-flux on the surface of the specimen and mounted on a Au plate with Ag paste. The XES measurements were performed at the undulator beamline BL-2C in KEK-PF.¹⁶⁾ The incident photon energy is about 400 eV. Emitted photons were detected using the MCP detector combined with the 1200 lines/mm grating. The energy resolution of the spectrometer with the slit width of 20 μ m was estimated as about $\Delta E \sim 0.2$ eV at the energy of $E = 200$ eV.¹⁷⁾ Polarization dependence of emission spectra on the angle between the *c*-axis and the detector-direction θ was measured at room temperature (Fig. 1). The XAS measurements were performed at BL-19B in KEK-PF by the total fluorescence yield (TFY) method. The energy resolution of the incident photon was about 0.2 eV. The geometry of XAS measurement was the same as that of the XES measurement.

In our experimental geometry, the fluorescence intensity with the incidence angle θ , $I^{\text{fluo}}(\theta)$, is expressed using PDOS components parallel to the $p\sigma$ and $p\pi$ orbitals, $I_{p\sigma}^{\text{fluo}}$ and $I_{p\pi}^{\text{fluo}}$

^{*}E-mail: jin@pc.uec.ac.jp

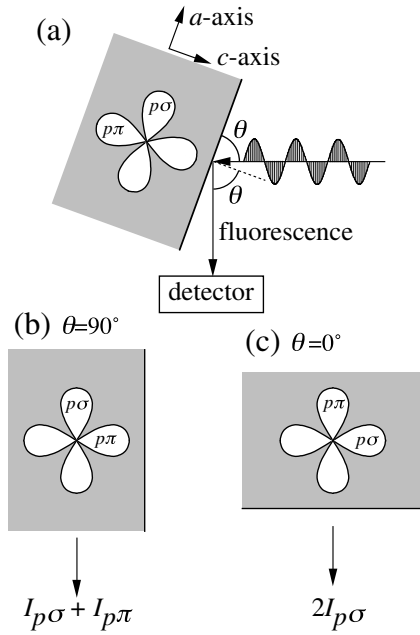


Fig. 1. (a) Experimental setup for soft X-ray emission spectroscopy. The hatched area shows the cross section of the hexagonal plate, i.e., *ac*-plane. Both the B- $2p\sigma$ and $2p\pi$ orbitals in the plane are shown. In addition to these orbitals, there is another $p\sigma$ component perpendicular to the plane. (b) In the case of $\theta = 90^\circ$, we observe the emission from both $p\sigma$ and $p\pi$ orbitals with equal weight. (c) In the case of $\theta = 0^\circ$, we observe $p\sigma$ -emission only.

because of the dipole transition (radiation) from B- $2p$ to $1s$ states;

$$I^{\text{fluo}}(\theta) = [1 + \cos^2(\theta)]I_{p\sigma}^{\text{fluo}} + \sin^2(\theta)I_{p\pi}^{\text{fluo}}. \quad (1)$$

Therefore, an ideal XES spectrum $I^{\text{fluo}}(0^\circ)$ contains only the $p\sigma$ component, and $I^{\text{fluo}}(90^\circ)$ contains both the $p\sigma$ and $p\pi$ components with equal weight.

We first show the theoretical PDOS of $p\sigma$ and $p\pi$ orbitals of MgB₂ and AlB₂ derived from band calculation (Fig. 2).¹⁵⁾ It is found that the overall feature of PDOS of MgB₂ is almost the same as that of AlB₂, i.e., the rigid band model

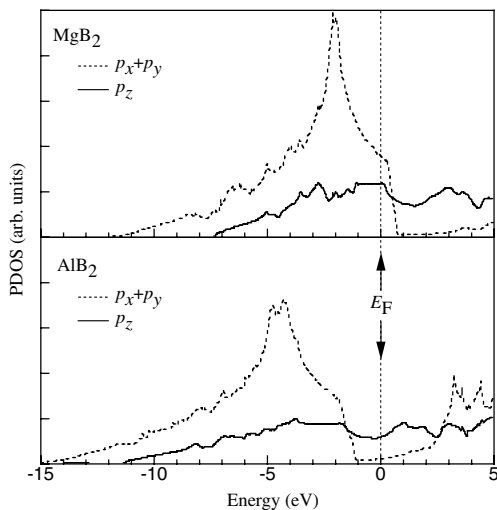


Fig. 2. Theoretical partial density of states of $p_x + p_y (= 2 \times p\sigma)$ and $p_z (= p\pi)$ orbitals in MgB₂ and AlB₂ derived from the FLAPW method.¹⁵⁾

roughly represents these materials. This is consistent with the previous XAS and XES results for the polycrystalline samples.⁴⁾ To be more precise, the detailed form of PDOS of MgB₂ is sharp in comparison with that of AlB₂, i.e., the peak of the $p\sigma$ band of MgB₂ at $E = -2$ eV is relatively sharp compared with that of AlB₂ at $E = -4.5$ eV. This is due to a reduction of two-dimensionality of B- p bands in AlB₂, which is consistent with the decrease of the lattice-constant ratio from MgB₂ ($c/a = 1.14$) to AlB₂ ($c/a = 1.08$). As mentioned in the introduction, an important difference between MgB₂ and AlB₂ predicted theoretically is that the Fermi energy lies within the $p\sigma$ band in the former, but not in the latter.

We now move on to the experimental results. Figure 3 shows the partial density of states (PDOS) of B- $2p\sigma$ and $2p\pi$, $I_{p\sigma}^{\text{fluo}}$ and $I_{p\pi}^{\text{fluo}}$, derived from observed $I^{\text{fluo}}(20^\circ)$ and $I^{\text{fluo}}(45^\circ)$. A self-absorption correction was applied to the observed XES spectra before the derivation of $I_{p\sigma}^{\text{fluo}}$ and $I_{p\pi}^{\text{fluo}}$. The area intensities of $I_{p\sigma}^{\text{fluo}}$ and $I_{p\pi}^{\text{fluo}}$ are normalized to unity in the energy region below 188 eV, and the $2I_{p\sigma}^{\text{fluo}}$ and $I_{p\pi}^{\text{fluo}}$ are shown in the figure. The value of E_F is about 187.5 eV which is about 1.5 eV higher than the value of MgB₂ (186 eV), which is in good agreement with the previous report for the polycrystalline AlB₂ sample.⁴⁾ It is clearly seen that there is almost no PDOS in $p\sigma$ orbitals of AlB₂ near E_F . Furthermore, there is a considerable amount of PDOS in $p\pi$ orbitals of AlB₂ around E_F .

Figure 4 shows the PDOS of B- $2p\sigma$ and $p\pi$, $2 \times I_{p\sigma}^{\text{abs}}$ (○) and $I_{p\pi}^{\text{abs}}$ (●), derived from observed absorption spectra $I^{\text{abs}}(20^\circ)$ and $I^{\text{abs}}(70^\circ)$. Similarly to the XES spectra, the self absorption correction was applied before their derivation, and the normalized absorption intensity $I^{\text{abs}}(\theta)$ is expressed as follows;

$$I^{\text{abs}}(\theta) = \sin^2(\theta)I_{p\sigma}^{\text{abs}} + \cos^2(\theta)I_{p\pi}^{\text{abs}}. \quad (2)$$

In PDOS of $p\pi$ [Fig. 4(a)], there is large absorption at about 194 eV in contrast to no sharp absorption in $p\sigma$ -PDOS, which is assigned to the $p\pi$ resonance state on the sample

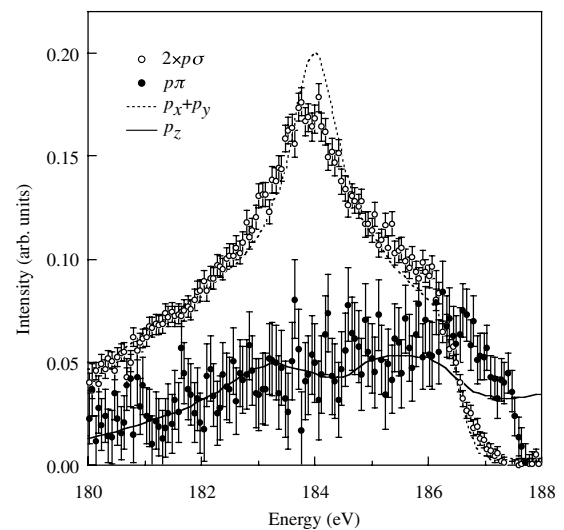


Fig. 3. Partial density of states (PDOS) of B- $2p\sigma$ and $p\pi$, $2 \times I_{p\sigma}^{\text{fluo}}$ (○) and $I_{p\pi}^{\text{fluo}}$ (●), derived from observed $I^{\text{fluo}}(20^\circ)$ and $I^{\text{fluo}}(45^\circ)$. Dotted and solid lines are the theoretical PDOS of $p_x + p_y (= 2 \times p\sigma)$ and $p_z (= p\pi)$ orbitals derived from band calculation (FLAPW) for AlB₂.¹⁵⁾

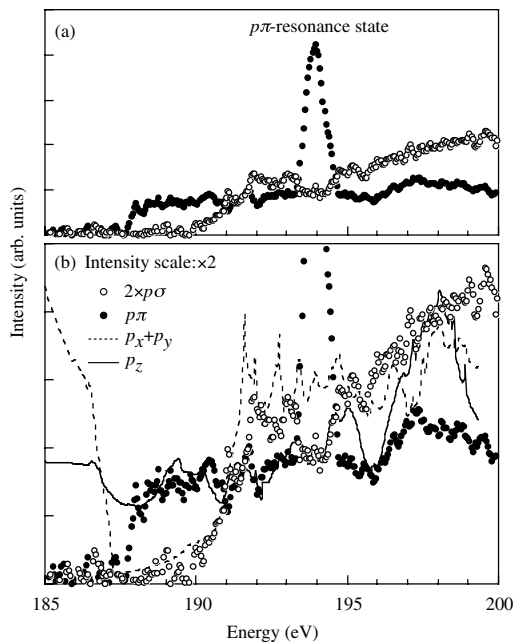


Fig. 4. Partial density of states (PDOS) of B- $2p\sigma$ and $p\pi$, $2 \times I_{p\sigma}^{\text{abs}}$ (○) and $I_{p\pi}^{\text{abs}}$ (●), derived from observed absorption spectra $I_{p\sigma}^{\text{abs}}(20^\circ)$ and $I_{p\pi}^{\text{abs}}(70^\circ)$: (a) Overall feature of PDOS and (b) comparison with the band calculation. Dotted and solid lines are the theoretical PDOS of $p_x + p_y (= 2 \times p\sigma)$ and $p_z (= p\pi)$ orbitals derived from band calculation (FLAPW) for AlB_2 .

surface.³⁾ In both figures (Figs. 3 and 4), the theoretical PDOS of AlB_2 are shown again by the dotted line ($p\sigma$) and the solid line ($p\pi$). It is found that the theoretical PDOS reproduces the observed PDOS well, for both the empty and occupied states. We have clearly observed a pseudo-gap of about 3 eV around 187–190 eV in the B- $2p\sigma$ orbital in sharp contrast to the broad metallic state of the B- $2p\pi$ orbital. The pseudo-gap is attributed to the bonding and anti-bonding state separation due to the strong covalent nature of $p\sigma$ orbitals.¹⁵⁾ However, there is a small difference in the value of E_F between the experimental and theoretical PDOS. The band calculation predicts the energy of $p\sigma$ -shoulder at about -1.8 eV below the Fermi level. However the observed energy of the shoulder (186.3 eV) locates -1.2 eV below the Fermi level (187.5 eV), i.e., the observed Fermi energy E_F is 0.6 eV lower than the theoretical prediction. The reason for this difference is considered to be the lack of Al atoms from the stoichiometry. The observed pseudo-gap in $p\sigma$ -PDOS at around the Fermi energy suggests the strong covalent bonding feature of boron forming the 2D honeycomb plane as reported by maximum entropy method (MEM)/Rietvelt analysis.^{18,19)} We considered that the layered B-honeycomb plane is the fundamental structure of AlB_2 . There is a small difference in electronegativity between Al and B atoms, so electrons transfer from Al to B atoms in AlB_2 compound. Vacancies of Al atoms in AlB_2 reduce the number of electrons of B- $2p$ orbitals, thus the Fermi levels shifts down. If we assume that the decrease of the states below E_F is due to an Al vacancy, the vacancy concentration x of $\text{Al}_{1-x}\text{B}_2$ is estimated to be about 0.07. The theoretical band calculation suggests that the heat of formation of AlB_2 is lower than that

of MgB_2 , which suggests the compound which has a lower number of electrons of the cation than the stoichiometric AlB_2 is more stable. The present result is consistent with this prediction.

To summarize, we have performed direct measurement of partial density of states (PDOS) of B- $2p$ bands in single-crystalline AlB_2 using polarization-dependent XES and XAS. We have clearly observed a pseudo-gap of about 3 eV in the B- $2p\sigma$ orbital in sharp contrast to the broad metallic state of the B- $2p\pi$ orbital. Although the experimentally observed PDOS is in excellent agreement with the band calculation results, the Fermi level in the former is found to be lower by about 0.6 eV than in the latter. Nevertheless, the Fermi level still lies well above the $p\sigma$ band, providing a direct confirmation that there are no $p\sigma$ holes in AlB_2 . Conversely, considering the fact that AlB_2 is not superconducting, our result indirectly supports scenarios that the $p\sigma$ holes play an important role in the occurrence of superconductivity in MgB_2 .

We express our thanks to Professor J. Akimitsu of Aoyama Gakuin University for useful discussions. We also thank to Mr. T. Takeuchi and Ms. A. Fukushima of ISSP for their technical support in the spectroscopic measurements. T.O. gratefully acknowledges the support by a Grant-in-Aid for COE Research (No. 13CE2002) of the Ministry of Education, Culture, Sports, Science and Technology of Japan. This experiment was performed under the approval of the Photon Factory Advisory Committee (Proposal No. 2001U004).

- 1) J. Nagamatsu, N. Nakagawa, T. Muranaka, Y. Zenitani and J. Akimitsu: *Nature (London)* **410** (2001) 63.
- 2) Z. Kurmaev, I. I. Lyakhovskaya, J. Kortus, N. Miyata, M. Demeter, M. Neumann, M. Yanagihara, M. Watanabe, T. Muranaka and J. Akimitsu: *cond-mat/0103487*.
- 3) T. A. Callcott, L. Lin, G. T. Woods, G. P. Zhang, J. R. Thompson, M. Paranthaman and D. L. Ederer: *Phys. Rev. B* **64** (2001) 132504.
- 4) J. Nakamura, N. Yamada, K. Kuroki, T. A. Callcott, D. L. Ederer, J. D. Denlinger and R. C. C. Perera: *Phys. Rev. B* **64** (2001) 174504.
- 5) M. Imada: *J. Phys. Soc. Jpn.* **70** (2001) 1218.
- 6) K. Yamaji: *J. Phys. Soc. Jpn.* **70** (2001) 1476.
- 7) J. Kortus, I. I. Mazin, K. D. Belashchenko, V. P. Antropov and L. L. Boyer: *Phys. Rev. Lett.* **86** (2001) 4656.
- 8) K. D. Belashchenko, M. van Schilfgaarde and V. Antrov: *Phys. Rev. B* **64** (2001) 092503.
- 9) G. Satta, G. Profeta, F. Bernardini, A. Continenza and S. Massidda: *Phys. Rev. B* **64** (2001) 104507.
- 10) J. M. An and W. E. Pickett: *Phys. Rev. Lett.* **86** (2001) 4366.
- 11) A. Reyes-Serrato and D. H. Galván: *cond-mat/0103477*.
- 12) S. Suzuki, S. Higai and K. Nakao: *J. Phys. Soc. Jpn.* **70** (2001) 1206.
- 13) H. Rosner, W. E. Pickett, S.-L. Drechsler, A. Handstein, G. Behr, G. Fuchs, K. Nenkov, K.-H. Müller and H. Eschrig: *Phys. Rev. B* **64** (2001) 144516/1-6.
- 14) N. I. Medvedeva, A. L. Ivanovskii, J. E. Medvedeva and A. J. Freeman: *Phys. Rev. B* **64** (2001) 020502.
- 15) T. Oguchi: unpublished.
- 16) M. Watanabe, A. Toyoshima, J. Adachi and A. Yagishita: *Nucl. Inst. Meth. Phys. Res. A* **467–468** (2001) 512.
- 17) Y. Harada, H. Ishii, M. Fujisawa, Y. Tezuka, S. Shin, M. Watanabe, Y. Kitajima and A. Yagishita: *J. Synchrotron Radiat.* **5** (1998) 1013.
- 18) E. Nishibori, M. Takata, M. Sakata, H. Tanaka, T. Muranaka and J. Akimitsu: *J. Phys. Soc. Jpn.* **70** (2001) 2252.
- 19) S. Lee, H. Mori, T. Masui, Y. Eltsev, A. Yamamoto and S. Tajima: *J. Phys. Soc. Jpn.* **70** (2001) 2255.